Spin dynamics in the paramagnetic phase of $YBa_2Cu_3O_{6.12}$ as seen by Cu NMR

R. Pozzi, M. Mali, and D. Brinkmann
Physik-Institut, Universität Zürich, CH-8057 Zürich, Switzerland

A. Erb
Département de Physique de la Matière Condensée, Université de Genève, 24, quai Ernest Ansermet, 1211 Genève 4, Switzerland

(Received 11 March 1999)

We report a Cu nuclear magnetic resonance (NMR) study at both Cu sites in the paramagnetic phase of $YBa_2Cu_3O_{6.12}$. By measuring the temperature dependence of the magnetic shift and the spin-lattice relaxation time, we have obtained the following major results. Above 500 K, the compound is in the renormalized classical regime of a two-dimensional quantum Heisenberg antiferromagnet (AF) with spin $S=1/2$. We have determined the temperature dependence of the AF correlation length, a value for the hyperfine coupling constant at the plane Cu(2) site, $|A_{ab}-4B|=117(3)$ kOe/μ_B, and the effective magnetic moment, $\mu_{\rm eff}=0.68(2)\mu_B$. Below 500 K, the individual layers start to couple into pairs and the temperature dependence of the AF correlation length abruptly crosses over to a faster increase when T_N is approached; the corresponding effective AF in-plane coupling constant becomes $J_{\rm eff}=4100$ K. A comparison with quantum Monte Carlo calculations allows one to estimate an intrabilayer coupling constant, $J_b/J\lesssim 0.01$, which is significantly smaller than $J_b/J=0.08$ as obtained by neutron-scattering experiments. Only ≈ 4 K above T_N, also the bilayers begin to couple. A further crossover has been observed in the Cu(2) spin-fluctuation symmetry: from XY-like fluctuations around T_N to isotropic fluctuations at ≈ 500 K. Due to its high value, T_N does not depend on the orientation of the applied magnetic field of 5.16 T. [S0163-1829(99)04137-5]

I. INTRODUCTION

The bilayered structure $YBa_2Cu_3O_6$ (YBCO6) is the antiferromagnetic (AF) parent compound of the $YBa_2Cu_3O_{6+y}$ superconductors (for $y>0.4$);[1] its Néel temperature T_N, is about 415 K. The investigation of the magnetic properties of YBCO6 is driven by two main interests. First, there is the question about a possible interplay between magnetism and superconductivity. Even if there is no direct relation between magnetism and the mechanism of superconductivity, magnetism in these compounds certainly reflects the strong electronic correlation that exists and that must be taken into account in any attempt to explain electron pairing in cuprates. Second, a bilayered AF offers insight into the crossover region between two-dimensional (2D) and three-dimensional (3D) magnetic systems.

In the paramagnetic phase of the quasi-2D *single-layer* antiferromagnets La_2CuO_4 (LACO) and $Sr_2CuO_2Cl_2$ (SCOCL), the critical spin dynamics has been extensively studied by neutron scattering[2,3] and nuclear magnetic or quadrupole resonance[4–9] and could be described successfully with the nonlinear σ model for a so-called *2D quantum Heisenberg AF with spin* $S=1/2$ (2D-QHAF for short).[10,11] For the *bilayered* system, an extended nonlinear σ model[12] and Monte Carlo simulations[12,13] predict a considerably different low-energy excitation spectrum. These results never have been verified experimentally before.

In this paper, we report such a study, by nuclear magnetic resonance (NMR), of YBCO6 which became feasible after high-quality single crystals are now available.[14,15] Our small single crystals (≈ 10 mg) are grown from a high-temperature solution and contain nearly no defects and impurity phases compared to the huge (≈ 10 g) porous melt-textured samples used in neutron-scattering experiments. The single crystals allow NMR experiments of the paramagnetic phase of YBCO6 over a very wide temperature range from T_N up to almost 1000 K.

The well-known facts about the *ordered* phase of YBCO6 are as follows. Neutron-scattering experiments revealed a 3D AF lattice consisting of the Cu(2) magnetic moments in the CuO_2 planes.[1] The magnetic moment arises from the hole in the $3d_{x^2-y^2}$ orbital ($S=1/2$) and lies parallel to the CuO_2 plane.[1,16] The Cu(1) ions residing between the bilayers are nonmagnetic ($S=0$). Although the magnetic lattice is 3D, the AF couplings are spatially very anisotropic: The superexchange interaction between nearest-neighbor (NN) spins in the plane (with coupling constant $J=1450$ K, Ref. 17) dominates both the *intra*bilayer ($J_b=0.08$ J, Ref. 17) and the *inter*bilayer coupling ($J'\approx 10^{-5}$ J, Ref. 1). These three couplings are assumed to be isotropic (Heisenberg coupling). However, in order to explain the preferred spin orientation parallel to the plane, a small XY anisotropy of J (that is $J_{xy}\approx 10^{-4}$ J, Ref. 1) has to be introduced. Thus, very close to T_N, YBCO6 should behave as a 3D-XY-AF.

Our Cu NMR study of both Cu sites in the *paramagnetic* phase of YBCO6 is a very detailed investigation of the spin dynamics. We are dealing with, among others, (i) the determination of the planar correlation length in the renormalized classical regime; (ii) the rapid increase of the correlation length below 500 K and the determination of an effective AF in-plane coupling constant; (iii) the crossover from isotropic Cu(2) spin fluctuations at high temperature to XY-like fluctuations around T_N; (iv) the reduction of the Cu(2) magnetic moment due to quantum fluctuations and its relation to the number of layers; (v) the effect of the motion of remnant

oxygen in the chains; and (vi) a possible explanation of the unusual increase of the ^{89}Y relaxation rate, measured previously, with rising temperature.

The paper is organized as follows. After briefly providing experimental details in Sec. II and the theoretical background of the experiment in Sec. III, we will present and analyze our data in Sec. IV. We will separately discuss the results from Cu(2) and Cu(1) NMR and will address topics which are typical for the various temperature regimes.

II. EXPERIMENTAL

The $YBa_2Cu_3O_{6+y}$ single crystals of ≈ 10 mg mass were grown using the recently developed $BaZrO_3$ crucibles[14] which, in contrast to other container materials, do not contaminate the growing crystal. Thus, our crystals exhibit a superior purity of more than 99.995 at. %.[15] To fix the oxygen content close to $y=0$ (Ref. 18), the crystals were annealed at 740 °C in flowing argon (99.998%) for 100–280 h followed by fast cooling to room temperature. In order to avoid oxygen absorption during our experiments performed at high temperatures, the crystals were sealed in a thin quartz tube at 10^{-3} mbar vacuum (crystals 1 and 2) or at 1 bar argon atmosphere (crystal 3).

X-ray-diffraction[19] revealed the lattice constants $a=b=3.8591(7)$ Å and $c=11.7854(35)$ Å, and a chain oxygen content of $y=0.12(2)$. The existence of remnant chain oxygen can also be inferred indirectly from the relatively small lattice constant c (compare with Refs. 16,20) and the slightly reduced Néel temperature (407.5 – 410.3 K) compared to the maximum values reported in the literature ($T_N \gtrsim 415$ K, Refs. 1,21).

Our YBCO6 single crystals turned out to be unstable at high as well as at room temperature. Crystal 2 decayed at 680 K, among others, into Cu_2O (monovalent Cu) and the other crystals, after some weeks or months, fell apart into sheets probably due to the decomposition of remnant flux inclusions, e.g., CuO (bivalent Cu) and $BaCuO_2$.

A standard NMR pulse spectrometer was used with external magnetic fields of 5.16 and 9 T. In order to eliminate the pulse-induced ringing, an add-subtract phase-altering pulse sequence was employed, which allows the echo delay time, τ, to be chosen as short as 10 μs. The signals were obtained by Fourier transformation of the spin echos or the free induction decays. The spin-lattice relaxation time, T_1, was measured using the inversion-recovery pulse sequence. About 50 μs turned out to be the shortest measurable relaxation time. The deviation from the desired crystal orientation ($\mathbf{B}_{\mathrm{ext}} \| c$ or $\| ab$) has been determined to be less than 2°.

During the extremely long course of $1/T_1$ measurements, all our single crystals have been severely damaged, so an extension to spin-spin relaxation rate measurements awaits new single crystals.

III. THEORETICAL BACKGROUND OF THE EXPERIMENT

The Cu nuclear spins ($I=3/2$) interact with their electronic environment through quadrupolar (i.e., electric) and magnetic hyperfine couplings. In the presence of an applied magnetic field $\mathbf{B}_0$, the Hamiltonian of the Cu nuclear spin $\mathbf{I}$, having a gyromagnetic ratio γ_n and a quadrupole moment eQ, can be written as

$$\mathcal{H} = \mathcal{H}_{\mathrm{Zeeman}} + \mathcal{H}^{\mathrm{quadrupole}}_{\mathrm{hyperfine}} + \mathcal{H}^{\mathrm{magnetic}}_{\mathrm{hyperfine}} \tag{1}$$

with

$$\mathcal{H}_{\mathrm{Zeeman}} = -\gamma_n \hbar \mathbf{B}_0 \mathbf{I} \tag{2}$$

and, for axially symmetric site symmetry (as is the case of both Cu sites in YBCO6),

$$\mathcal{H}^{\mathrm{quadrupole}}_{\mathrm{hyperfine}} = \frac{eQV_{zz}}{4I(2I-1)}[3I_z^2 - I(I+1)]. \tag{3}$$

$\mathcal{H}^{\mathrm{magnetic}}_{\mathrm{hyperfine}}$ describes the *magnetic* coupling between $\mathbf{I}$ and its electronic environment.

Here, V_{zz} denotes the largest principal component of the electric-field gradient (EFG) tensor $\mathbf{V}$, which, for both Cu sites, is along the $\mathbf{c}$ axis. The quadrupolar frequency $\nu_Q \equiv eQV_{zz}/2h$ is a measure for the quadrupolar interaction energy.

The presence of $\mathcal{H}^{\mathrm{magnetic}}_{\mathrm{hyperfine}}$ in Eq. (1) results in a magnetic shift of the central line, i.e., the $m=1/2 \leftrightarrow -1/2$ transition. This frequency shift $\Delta\nu_{\mathrm{mag}}$ is measured with respect to the Cu Larmor frequency ν_{L}, determined in a diamagnetic reference substance such as CuCl. The *relative* magnetic shift is defined as $K = \Delta\nu_{\mathrm{mag}}/\nu_{\mathrm{L}}$ with the special value K_c if $\mathbf{B}_0$ is parallel to $\mathbf{c}$. For this orientation, there is no quadrupolar shift of the central transition frequency, hence $\Delta\nu_{\mathrm{mag}}$ can be evaluated directly from the measured frequency, thus allowing a very accurate determination of K_c.

The components of the magnetic shift tensor measured in the experiment $\mathbf{K}^{\mathrm{exp}}$, can be decomposed into a spin and an orbital part, for instance,

$$K_c^{\mathrm{exp}}(T) = K_c^{\mathrm{spin}}(T) + K_c^{\mathrm{orb}}. \tag{4}$$

In cuprates, the orbital part is anisotropic[22] and assumed to be temperature independent. The spin part, which is anisotropic as well but changes with temperature, can be expressed by the spin hyperfine coupling tensor and the temperature-dependent static electronic spin susceptibility. For the $\mathbf{c}$ component, we have

$$K_c^{\mathrm{spin}} = \frac{1}{g_c \mu_B} A_c^{\mathrm{spin}}(\mathbf{q}=0) \cdot \chi_{o,c}^{\mathrm{spin}}(T). \tag{5}$$

g_c, μ_B, and $\mathbf{q}$ denote the c component of the slightly anisotropic Cu^{2+} spectroscopic splitting factor, the Bohr magneton and the wave vector, respectively. According to Mila and Rice,[22] the $\mathbf{q}=0$ spin hyperfine coupling constant for the planar Cu(2) site can be written as $A_c^{\mathrm{spin}} = A_c + 4B$, where A_c is the $\mathbf{c}$ component of the anisotropic on-site hyperfine coupling tensor and B represents the transferred isotropic hyperfine coupling with one of the four Cu(2) NN spins in the plane. For the Cu(1) site, since there is no on-site spin, only a transferred hyperfine coupling (represented by B_c') with the two Cu(2) NN spins has to be taken into account. Thus $A_c^{\mathrm{spin}} = 2B_c'$.

In the whole temperature range examined, the Cu(2) spin-lattice relaxation is known to be caused by the fluctuations of the Cu(2) electron spins. Thus we obtained the spin-lattice

relaxation rate, $2W$ (or equivalently $1/T_1$), by fitting our magnetization recovery data, $M(t_w)$, of the central line to the theoretical expression for recovery due to *magnetic* relaxation (Ref. 23):

$$M(t)=M_0-C[0.9\exp(-12Wt_w)+0.1\exp(-2Wt_w)], \tag{6}$$

where t_w is the time elapsed after the application of the inversion pulse, M_0 is the equilibrium value, and C is a parameter depending on the excitation pulse.

General expressions for the relaxation rates, $2W_c=1/T_{1c}$ (for $\mathbf{B}_0\|c$ axis) and $2W_{ab}=1/T_{1ab}$ (for $\mathbf{B}_0\|ab$ plane), respectively, have been provided by Moriya:[24]

$$2W_c(T)=\frac{2\gamma_n^2k_BT}{2\mu_B^2}\sum_q (A_{ab}^{\rm spin}(\mathbf{q}))^2\frac{\chi''_{ab}(\mathbf{q},\omega_n,T)}{\omega_n}, \tag{7}$$

$$2W_{ab}(T)=\frac{\gamma_n^2k_BT}{2\mu_B^2}\sum_q\left[(A_{ab}^{\rm spin}(\mathbf{q}))^2\frac{\chi''_{ab}(\mathbf{q},\omega_n,T)}{\omega_n}+(A_c^{\rm spin}(\mathbf{q}))^2\frac{\chi''_c(\mathbf{q},\omega_n,T)}{\omega_n}\right], \tag{8}$$

where $A_{\alpha\alpha}^{\rm spin}(\mathbf{q})$ and $\chi''_{\alpha\alpha}(\mathbf{q})$ ($\alpha\alpha=ab,c$) are the wave-vector-dependent spin hyperfine coupling constant and imaginary part of the electron spin susceptibility, respectively, and ω_n denotes the nuclear precession frequency.

Due to the AF correlations, the susceptibility in YBCO6 is enhanced at the AF wave vector, $\mathbf{Q_{AF}}=(\pi/a,\pi/a)$, and exhibits, at this vector, a strong peak. Therefore, the predominant part of the spin-lattice relaxation comes from the spin fluctuations with wave vectors at and close to $\mathbf{Q_{AF}}$. By assuming at $\mathbf{Q_{AF}}$ a slow change of $A_{\alpha\alpha}^{\rm spin}(\mathbf{q})$ as compared to the sharply peaked $\chi''_{\alpha\alpha}(\mathbf{q})$, we approximate, in Eqs. (7) and (8), $A_{\alpha\alpha}^{\rm spin}(\mathbf{q})$ by $A_{\alpha\alpha}^{\rm spin}(\mathbf{Q_{AF}})$. For Cu(2), the hyperfine coupling constant at $\mathbf{Q_{AF}}$ is $(A_{\alpha\alpha}-4B)$ and the $(A_{\alpha\alpha}^{\rm spin})^2$ value for the Cu(1) site equals 0 or $2(B'_{\alpha\alpha})^2$, depending on whether the spins of adjacent bilayers fluctuate AF coupled or not.

The width of the susceptibility peak is isotropic since it is determined by the inverse of the isotropic AF correlation length, $\xi(T)$ (see, for example, the Millis, Monien, and Pines model[25]). Therefore, together with the approximation $A_{\alpha\alpha}^{\rm spin}(\mathbf{q})\approx A_{\alpha\alpha}^{\rm spin}(\mathbf{Q_{AF}})$, the temperature dependence of the spin-lattice relaxation rate anisotropy can be related to the anisotropy of χ'' at the AF wave vector in the following way.

We define a *susceptibility anisotropy factor* κ by

$$\kappa(T)=\frac{2W_{ab}(T)-W_c(T)}{W_c(T)}\approx\frac{(A_c^{\rm spin}(\mathbf{Q_{AF}}))^2}{(A_{ab}^{\rm spin}(\mathbf{Q}_{AF}))^2}\cdot\frac{\chi''_c(\mathbf{Q_{AF}},T)}{\chi''_{ab}(\mathbf{Q_{AF}},T)}. \tag{9}$$

This definition is useful for two reasons. First, the anisotropy of the hyperfine coupling constant at $\mathbf{Q_{AF}}$ can be determined. Since the spins fluctuate isotropically far above T_N, the ratio χ''_c/χ''_{ab} equals the constant value $(g_c/g_{ab})^2\approx1.2$ (Refs. 20,24,26,27). Thus, κ yields, at high temperatures, the ratio $|A_c^{\rm spin}(\mathbf{Q_{AF}})/A_{ab}^{\rm spin}(\mathbf{Q_{AF}})|$. Second, since one generally assumes the hyperfine coupling constants to be temperature independent, measuring κ now allows us to determine the temperature dependence of the ratio $\chi''_c(\mathbf{Q_{AF}})/\chi''_{ab}(\mathbf{Q_{AF}})$ thus providing direct information on the asymmetry of the Cu(2) spin fluctuations.

We now turn to the spin-lattice relaxation of Cu(1) where two different regimes must be distinguished. Below ≈500 K, the relaxation is mainly due to magnetic fluctuations whereas above ≈500 K, fluctuations of the electric-field gradient due to the motion of remnant chain oxygen are dominant. In case of purely quadrupolar relaxation, the echo recovery of the central line is given by[28]

$$M(t_w)=M_0-C[0.5\exp(-2W_1t_w)+0.5\exp(-2W_2t_w)], \tag{10}$$

where $2W_1$ and $2W_2$ represent the quadrupolar relaxation rates due to $\Delta m=1$ and $\Delta m=2$ transitions, respectively. Since the permutation of $2W_1$ and $2W_2$ in Eq. (10) yields the same relaxation law, the fit result does not tell which is the $2W_1$ and $2W_2$ term, respectively.

We assume the diffusing oxygen ions to move only in the Cu(1) plane. For such a motion, they produce a fluctuating EFG tensor whose V_{xz} and V_{yz} components are zero at the Cu(1) site in a frame with z perpendicular to the Cu(1) plane ($z\|c$). Therefore, when an external magnetic field (defining the quantization axis, z) is applied along the c axis (as in our experiment), the lack of V_{xz} and V_{yz} components, for this special field orientation, leads to $2W_1=0$ (Refs. 29 and 30). Thus, we regard $2W_2$ to be the larger value of the two Cu(1) rates.

IV. EXPERIMENTAL RESULTS AND DISCUSSION

A. Cu(2) spin-lattice relaxation

In the whole temperature range we studied, Cu(2) nuclei relax due to the AF electron-spin fluctuations. Thus, the temperature dependence of the spin-lattice relaxation time offers an excellent opportunity to study the low-energy excitations of a bilayer QHAF with weak coupling between the planes, that is $J_b/J<0.1$. We will start with presenting the data followed by a discussion of the effects studied in the various temperature regimes.

1. Experimental data

Because of occasional decomposition of the YBCO6 single crystals at high temperatures, we had to perform relaxation measurements on three different specimens (see Sec. II), partially in different, though overlapping temperature regions (see Fig. 1). Whenever comparison is possible, the experimental $1/T_1$ values of different crystals turned out to agree within 15%. At 670 K, far above T_N, crystal 3 with the lowest T_N has also the lowest $1/T_{1c}$, suggesting a slight decrease of $1/T_{1c}$ with lower T_N. On the other hand, the $1/T_{1c}$ measured by Mali *et al.*[31] on oriented YBCO6 powder with $T_N=416$ K that surpasses all single crystals T_N, is not higher but about 20% *lower* than the single-crystal value. Thus, there is no clear trend of $1/T_{1c}$ far above T_N as compared to the small differences in T_N. Most of the experimen-

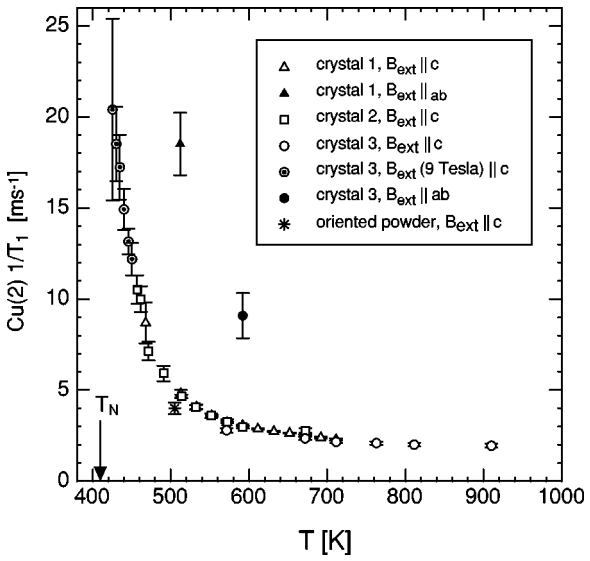

FIG. 1. Temperature dependence of the plane Cu(2) spin-lattice relaxation rate in three different $YBa_2Cu_3O_{6.12}$ single crystals with the external magnetic field of 5.16 T (except for the crystal 3 measurements close to T_N) either parallel or perpendicular to the c axis. The star denotes a value measured on oriented $YBa_2Cu_3O_6$ powder (Ref. 31). The same symbols will be used throughout the following graphs unless otherwise stated. The Néel temperature is denoted by the arrow.

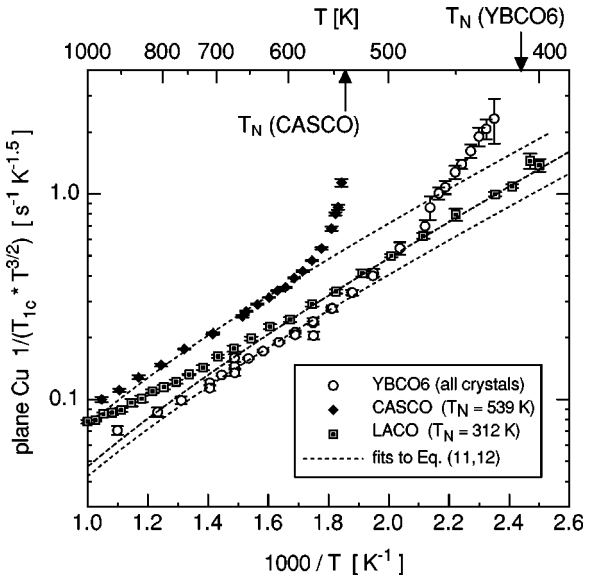

FIG. 2. Temperature dependence of Cu(2) $1/(T_{1c}\cdot T^{3/2})$ in $YBa_2Cu_3O_{6.12}$ (this work), $(Ca,Sr)CuO_2$ (Ref. 34), and La_2CuO_4 (Ref. 7). The dashed lines are fits to the data using the model of a $S=1/2$ 2D quantum Heisenberg antiferromagnet in the renormalized classical regime.

tal data were determined in a magnetic field, $B_{\text{ext}}=5.16$ T, except for the crystal 3 data close to T_N which were measured at 9 T to benefit from a better signal-to-noise ratio. Unfortunately, the operating temperature of this magnet's cryostat is limited to 450 K. Since the temperature dependence of the 5.16 and 9 T data connect smoothly, we assume in the following that $1/T_1$ is independent of B_{ext}.

2. Renormalized classical regime

At temperatures far enough above T_N, where the interplane couplings, J_b and J', play a minor role in the spin dynamics, the measured $1/T_{1c}$ can be compared with the theoretical predictions of the nonlinear σ model for a 2D-QHAF (with $S=1/2$) in the so-called renormalized classical (RC) regime. This regime is governed by the critical slowing down of the spin fluctuations if the temperature approaches the ordering temperature, $T_N^{2D}=0$, of an ideal 2D-QHAF. In the RC regime, the low-energy spin dynamics are described in terms of the spin-wave stiffness constant ρ_S, and the spin-wave velocity, both being linear functions of the intraplanar coupling constant, J.[11] According to this model, the relaxation rate $1/T_{1c}$ and the planar spin-correlation length, ξ_{2DH} (normalized, as usually, to the lattice constant a), are related to each other as follows:[10,11]

$$1/T_{1c}(T)=0.3\frac{(A_{ab}-4B)^2}{J\hbar}\xi_{2DH}(T)\frac{x^{3/2}}{(1+x)^2}, \qquad (11)$$

$$\xi_{2DH}(T)=0.5\ \exp(1/x)[1-(x/2)+O(x^2)], \qquad (12)$$

where $x=T/(1.13J)$. Hence, the temperature dependence of $1/T_{1c}$ is dominated by the term $T^{1.5}\exp(1.13J/T)$. In the temperature range 520–700 K, the predicted curves for RC behavior agree quite well with our experimental data, see Fig. 2. In principle, the fit of Eqs. (11) and (12) to the data allows for two fit parameters, J and $|A_{ab}-4B|$. However, since $1/T_{1c}(T)$ is much less sensitive to variations of J than to those of $|A_{ab}-4B|$, we decided to use only the hyperfine coupling constant as a fit parameter and to take $J=1450$ K as determined by neutron scattering.[17] The best fit yields $|A_{ab}-4B|=117(3)$ kOe/μ_B.

Following the analysis introduced by Imai *et al.*[5] the known value of $|A_{ab}-4B|$ allows us to determine the effective magnetic moment μ_{eff} via the relation $B_{\text{int},0}=|A_{ab}-4B|\mu_{\text{eff}}$, where $B_{\text{int},0}$ is the internal magnetic field measured in the ordered phase at very low temperatures. We perform this determination not only for YBCO6 but also for LACO and for the infinite-layer compound $(Ca,Sr)CuO_2$ (CASCO) whose relevant parameters, together with the results, are listed in Table I. CASCO, which exhibits nearly 3D behavior,[32] has a larger moment than the bilayered YBCO6 whose moment, in turn, is larger than that of the single-layered LACO where all planes are coupled only extremely weakly.[1] These findings agree qualitatively with theoretical results[33] obtained for a single-, bi- and infinite-layered AF system (Table I). The moments evaluated for YBCO6 and CASCO are smaller than the corresponding theoretical values because the latters have been calculated for the special case of spatially isotropic AF coupling, i.e., $J'=J_b=J$. Thus, the value of the effective magnetic moment increases with increasing number of layers; this confirms the general statement that quantum fluctuations play a minor role in systems of higher dimension.

3. Deviations from the RC behavior at high temperatures

There are two temperature regimes where $1/T_{1c}$ departs from the curves predicted for RC behavior. We will first discuss the regime above ≈ 700 K, where the $1/T_{1c}$ rates in

TABLE I. Relevant parameters of YBCO6 and related antiferromagnets.

	CASCO	YBCO6	LACO
J (K)	1450(150) (Ref. 34)	1450 (Ref. 17)	1550(50) (Ref. 53)
$\lvert A_{ab}-4B\rvert$ (kOe/μ_B)	155(10) (Ref. 34)	117(3)	122(2) (Ref. 53)
$B_{int}(T\rightarrow 0)$ (kOe)	115.2 (Ref. 32)	79.65 (Ref. 54)	78.78 (Ref. 55)
μ_{eff} (μ_B) *evaluated*	0.74(5)	0.68(2)	0.645(10)
μ_{eff} (μ_B) *theoretical*	0.82 (Ref. 33)	0.73 (Ref. 33)	0.61 (Ref. 33)

all three compounds, YBCO6, CASCO (Ref. 34) and LACO (Ref. 7), are shifted to values higher than the curves for RC behavior (see Fig. 2).

One possible explanation of the observed deviations at high temperatures is the spin diffusion which adds a long wavelength ($\mathbf{q}\rightarrow 0$) contribution to the relaxation rate. In LACO, it might amount up to 10% of the whole relaxation rate at 900 K and is proportional to the square of the $\mathbf{q}=0$ hyperfine coupling constant, $(A_{ab}+4B)^2$.[35] In CASCO, this quantity has the value 9000 $(\mathrm{kOe}/\mu_B)^2$ (Ref. 34), which is distinctly smaller than 26 400 and 36 200 $(\mathrm{kOe}/\mu_B)^2$ in LACO and YBCO6, respectively.[36] Thus, one would expect a spin-diffusion contribution, and hence a deviation from the RC behavior, that is about three times smaller in CASCO than those in LACO and YBCO6. However, the experiment revealing a more or less material-independent deviation does not support this explanation.

Another explanation option for the observed deviation could be the crossover from the RC regime to the so-called quantum critical regime at $T\approx J/2$ where $\xi_{2D}\propto 1/T$ and $1/T_1 \approx$const (Refs. 37 and 5–7) or the crossover to the high-temperature behavior where $1/T_1$, after passing through a minimum,[11] starts to grow towards the constant $1/T_{1,\infty}$ value.[38]

4. Bilayer correlation length

The other deviation from the curve for RC behavior, which occurs below 500 K (see Fig. 2), is interpreted as the signature of the coupling of the layers into pairs which can be regarded as new entities. To show this, we plot, in Fig. 3, an ''experimental'' correlation length, $\xi_{2D,exp}$, which we calculated by help of Eq. (11), which is valid quite generally,[11,12] using our $1/T_{1c}$ data, the value $\lvert A_{ab}-4B\rvert = 117$ kOe/μ_B (from the fit described above), and $J = 1450$ K (Ref. 17). Obviously, $\xi_{2D,exp}$ displays a kink around 500 K and deviates from the curve for RC behavior thus indicating the onset of intrabilayer coupling. It turns out that the data below 500 K can be fitted by the expression $\xi_{2D,exp}=C(1-x/2)\exp(1/x)$ with $x=T/1.13J_{eff}$ which, in this form, is essentially the same as Eq. (12) that is valid for a *single* isolated layer. The best fit delivers

$$C=1.14(80)\times 10^{-3} \quad \text{and} \quad J_{eff}=4120(300)\ \mathrm{K},$$

where J_{eff} is approximately *three times* the value of J. This temperature dependence below 500 K implies a divergence of the bilayer correlation length at $T_N^{2D}=0$ and is qualitatively different from the 3D critical increase of $1/T_1$ in CASCO at its finite Néel temperature, $T_N^{3D}=539$ K (see next section and Fig. 4).

We now compare our results with two theoretical treatments. Recently, Yin *et al.*[12] have calculated the correlation length for a *bilayer* AF. In Fig. 3, the dotted line is their result for the specific value in YBCO6, $J_b/J=0.08$, as obtained from neutron scattering.[17] This line obeys quite accurately the simple expression $\xi_{2D,bi}=C\exp(1.13J_{eff}/T)$ with $C=6.23(1.00)10^{-2}$ and $J_{eff}=3200(50)$ K. Compared with the two fits to our $\xi_{2D,exp}$ data below and above $T=500$ K, the slope of the ''Yin curve'' is too high at high temperatures and too low at temperatures close to T_N. In addition, the ''Yin curve'' does not display the crossover behavior observed at $T=500$ K and the absolute value of $\xi_{2D,exp}$ at 500 K is approximately one order of magnitude overestimated. Thus, the prediction for the bilayer structure in the RC regime is not as successful as that for the single-layer AF.

Next, we compare our data with quantum Monte Carlo (QMC) calculations[12,13] which have been performed to determine the correlation length for various values of the intrabilayer coupling, J_b. The results of the two groups are shown in Fig. 3 by dashed[13] and dashed-dotted[12] lines. The curve for $J_b=0$ confirms the analytical result of Eq. (12).

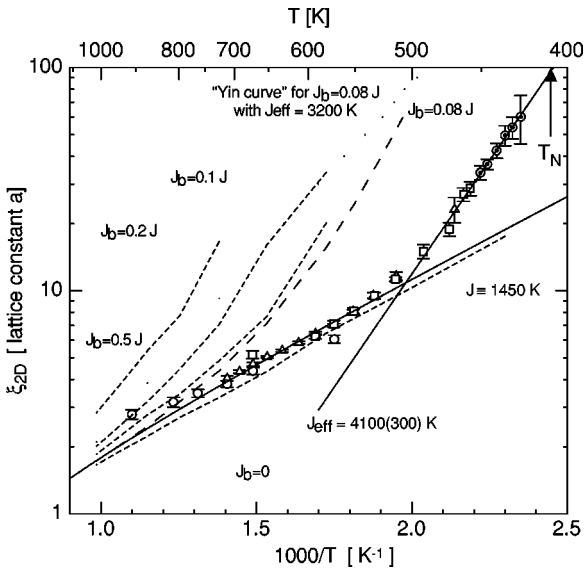

FIG. 3. The planar antiferromagnetic correlation length ξ_{2D} as a function of inverse temperature. The solid lines are fits to the experimental data above and below 500 K, respectively. The dotted line represents the prediction for a $S=1/2$ bilayer quantum Heisenberg antiferromagnet in the renormalized classical regime (Ref. 12) with $J_b/J=0.08$. The dashed (Ref. 13) and dashed-dotted (Ref. 12) curves are the results of quantum Monte Carlo calculations for bilayers with intrabilayer coupling constants, J_b, ranging from $0.08J$ to $0.5J$.

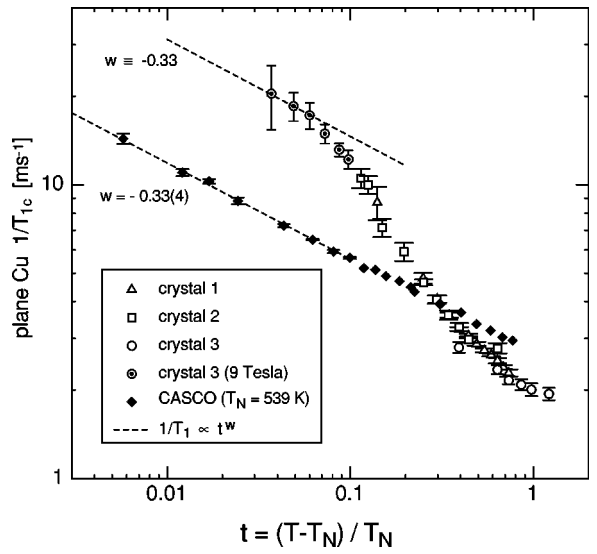

FIG. 4. The spin-lattice relaxation rate of plane Cu versus reduced temperature for $YBa_2Cu_3O_{6.12}$ (this work) and $(Ca,Sr)CuO_2$ (Ref. 34). The dashed lines represent a power-law behavior with a critical exponent w.

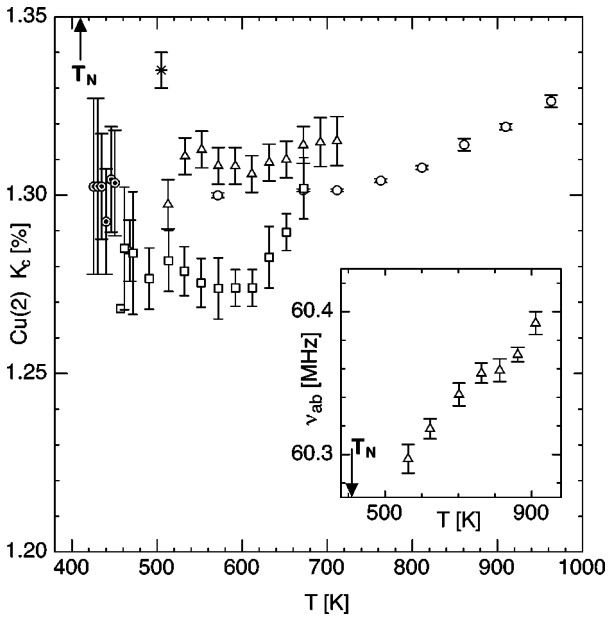

FIG. 5. Temperature dependence of the Cu(2) magnetic shift in c direction. Inset: Cu(2) central transition frequency versus temperature for the external field (5.16 T) parallel to ab.

The slopes of the other curves, for $J_b>0$, seem to approach, at high temperature, the slope of the single-layer curve, and approach approximately the slope of our data at low temperatures, as soon as the calculated ξ_{2D} value exceeds ≈ 10 lattice constants. However, the predicted curve for $J_b/J=0.08$ exhibits its ''kink'' at much higher temperature than our experimental curve.

The discrepancy may be solved by either assuming that the Hamiltonian used in the calculation has to be improved by taking into account, for instance, a next-nearest-neighbor coupling which markedly diminishes the correlation length or by postulating a much smaller bilayer coupling, for example $J_b/J \lesssim 0.01$. The apparent discrepancy with the neutron-scattering result, $J_b/J=0.08$, is not understood at present.

5. Critical behavior near T_N

In order to discuss the $1/T_{1c}$ data when the temperature approaches T_N^+, we plot the relaxation rate as a function of the reduced temperature, $t=(T-T_N)/T_N$, and include, for comparison, our previous Cu data[34] for CASCO, where $T_N=539$ K (Fig. 4). While the relaxation rate in CASCO exhibits 3D critical behavior over quite a large temperature range,[34] i.e., $1/T_{1c} \propto t^w$ with $w=-0.33(4)$, this is not the case for YBCO6. Only the three YBCO6 data points closest to T_N could signalize the onset of a critical behavior with $w \approx -0.33$. Unfortunately, technical reasons did not allow us to get closer to T_N than 15 K. Certainly, close enough to T_N, all 3D-XY-like AF are expected to display the same critical exponent w. The fact that the 3D critical temperature region in YBCO6 is barely detected and is so much smaller than that of CASCO, is a consequence of the very small interbilayer coupling, $J' \approx 10^{-5} J$ (Ref. 1) which is about three orders of magnitude weaker than the coupling between the CASCO layers.[32]

6. Anisotropy of the susceptibility

The Cu relaxation rate for $B_{ext} \| ab$, $1/T_{1ab}$, has been measured at two temperatures, $T=512$ and 592 K. For this orientation, the NMR signal is severely reduced because the line is broader and the spin-echo decay rate is very large. Together with the $1/T_{1c}$ data at 512 and 592 K, we obtain the following relaxation rate anisotropies: $T_{1c}/T_{1ab}=3.8(5)$ and 3.4(6), respectively. Within the error bars, this result implies that the anisotropy is temperature independent in this range, or in other words, the transition from XY-like spin fluctuations close to T_N to isotropic spin fluctuations far above T_N is already completed at about 500 K. Further support for this interpretation follows in Sec. IV C 4.

Our result $T_{1c}/T_{1ab}=3.8(5)$ confirms the 3.8 value determined for YBCO6 by Zha *et al.*[36] Furthermore, our value agrees, within the errors, with the anisotropy of 3.9(3) measured in LACO (Ref. 5). This similarity of the anisotropies supports the known fact that YBCO6 and LACO have similar A_c, A_{ab}, and B hyperfine coupling constants.[36]

The relaxation rate anisotropies allow one to calculate the susceptibility anisotropy factors κ, which are 6.6(1.0) and 5.8(1.2), respectively, at 512 and 592 K, and which are significantly larger than the CASCO value, $\kappa(950\ \mathrm{K})=3.7(2)$ (Ref. 34). At temperatures ≈ 100 K above T_N, κ depends only on the hyperfine coupling constants, therefore this difference in κ confirms our recent finding that the A_{ab} constant in CASCO quite strongly departs from those evaluated in YBCO6 and LACO. For the same reason, the hyperfine field in CASCO at $T \to 0$ is about 45% higher than those in YBCO6 and LACO (see Table I). This unusual A_{ab} value of CASCO reveals unambiguously that the electronic configuration of Cu in the CASCO plane differs considerably from those in LACO and YBCO6, presumably due to the absence of apical oxygen in CASCO.

B. Cu(2) magnetic shift and linewidth

Figure 5 shows the temperature dependence of the K_c component of the Cu(2) magnetic shift, measured at 5.16 T, for all three crystals together with some 9 T data for crystal 3 and the data point for oriented powder.[31] Note that, for the crystal samples, the K_c data fall into a very narrow range of only 0.06%. The minor differences in the absolute values of K_c for the different crystals are caused by minimal departures of less than 1.5° from the ideal $c \| B_{\text{ext}}$ crystal orientation.

Below 600 K, the magnetic shift in all samples is, within the error bar limits, temperature independent, and, in addition, there is no field dependence seen in crystal 3. The temperature independence of K_c is in accord with previous results for the superconductors $YBa_2Cu_3O_7$ (Ref. 39), $YBa_2Cu_4O_8$ (Ref. 40), and $La_{2-x}Sr_xCuO_4$ (Ref. 41) which implies that also for insulating YBCO6 the on-site and transferred contributions of the static spin hyperfine fields compensate to zero, that is $A_c + 4B \approx 0$.

However, above 600 K, the K_c data of all three crystals reveal a slight temperature dependence which starts at somewhat different temperatures and with slightly different slopes. The K_c increase, which is most clearly seen in crystal 3, does not reflect the temperature dependence of the static susceptibility whose slope diminishes when the temperature approaches 1000 K (Refs. 20,42,43). Therefore, according to Eqs. (4) and (5), the hyperfine coupling constants must change at high temperature.

A possible origin of such a change could be the excitement of the $3d$ hole into the next higher state, i.e., into the $3d_{3z^2-r^2}$ orbital. Such an excitation, however, would strongly affect the quadrupolar frequency ν_Q because it is extremely sensitive to a change of the charge distribution around the nucleus, and $\nu_Q(T)$ in turn mainly determines the temperature dependence of the resonance frequency ν_{ab}, measured for $\mathbf{B}_{\text{ext}} \| ab$. There is no strong temperature variation of ν_Q as seen by ν_{ab} (inset in Fig. 5) that exhibits only the usual increase with increasing temperature due to the thermal expansion of the crystal lattice.[32,34] Thus, a tentative hole excitement is excluded as the origin of the unusual increase of K_c at high temperatures. At present, we have no explanation for this unusual behavior.

Figure 6 displays the temperature dependence of the Cu(2) linewidth (defined as half width at half height). Very close to T_N, the line shape becomes asymmetric with a tail at the low-frequency side. Since the linewidth data of the individual crystals scatter considerably, we conclude that the linewidth we measured is not an intrinsic property of YBCO6, but depends strongly on the quality of the individual crystal.

At 505 K, the smallest linewidths are 85 and 170 kHz for the orientations $\mathbf{B}_{\text{ext}} \| c$ and $\mathbf{B}_{\text{ext}} \| ab$, respectively. Since these values are almost the same as observed in oriented powder,[31] the same statements made in that publication apply to the present single-crystal results. Quadrupolar broadening can be ruled out because, in such a case, the Cu(1) linewidth would be larger than the Cu(2) one because of the larger Cu(1) quadrupolar frequency (29.6 MHz compared to 23.8 MHz, Ref. 31). However, the corresponding Cu(1) linewidths we measured in our crystal at T_N are only 6 and 33 kHz.

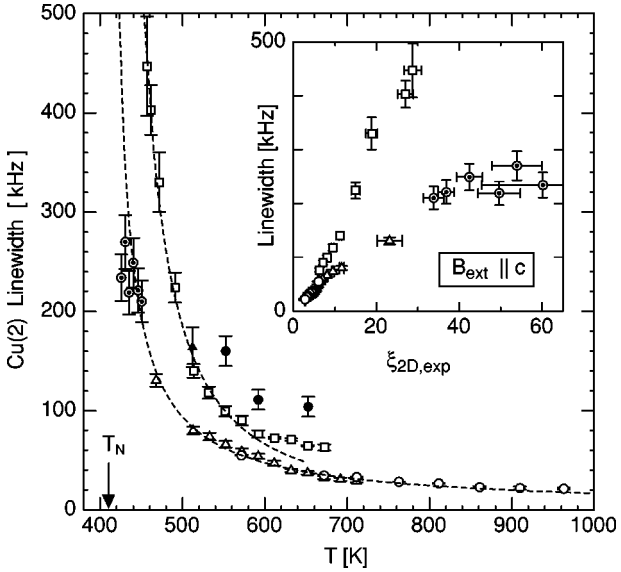

FIG. 6. Temperature dependence of the Cu(2) linewidth for $\mathbf{B}_{\text{ext}} \| c$ (open) and $\mathbf{B}_{\text{ext}} \| ab$ (full symbols). The dashed lines are fits to a tentative power-law behavior (see text). Inset: linewidth (for $\mathbf{B}_{\text{ext}} \| c$) versus planar antiferromagnetic correlation length.

The pronounced increase of the linewidth when T_N is approached from above, is *not* the result of 3D critical fluctuations as can be seen in the following way. We have tentatively fitted the temperature dependence by the ''critical equation'' $\textit{linewidth} = C(T - T_N)^p$ leading to a nice agreement with the data in the vicinity of T_N. However, for the two fit curves in Fig. 6, not only the two exponents, namely $p = -1.4(1)$ and $p = -0.9(1)$, disagree considerably, but also the two constants C differ by more than one order of magnitude. Therefore, 3D critical behavior does not describe satisfactory the linewidth data.

Instead, the linewidth can be related to the in-plane AF correlation length, $\xi_{\text{2D,exp}}$, as discovered for LACO by Imai *et al.*[6] The inset of Fig. 6 shows clearly that both quantities exhibit the same temperature dependence in the whole temperature range examined thus confirming that linewidth and correlation length are intimately related. Since the magnetically broadened linewidth is sample dependent there must be some sort of sample-dependent disorder or defects that enhance the magnetical broadening of the linewidth.

C. Cu(1) spin-lattice relaxation

Figure 7 gives a summary of the $1/T_{1c}$ Cu(1) spin-lattice relaxation rate data. One can distinguish temperature regimes with quite different relaxation behavior which we will discuss now.

1. Transferred hyperfine field at Cu(1) site

In the temperature range $T_N < T < 500$ K, the Cu(1) relaxation rate is about three orders of magnitude smaller than the Cu(2) relaxation rate. As shown in Fig. 8, Cu(1) and Cu(2) $1/T_{1c}$ have the same temperature dependence between 425 and 470 K (corresponding to the t range $4 \times 10^{-2} - 1.5 \times 10^{-1}$) with a scaling factor of $T_{1c,\text{Cu(1)}}/T_{1c,\text{Cu(2)}} = 2600$. Such a large difference of the rates can be accounted for only if the Cu(1) ion by itself does not possess an un-

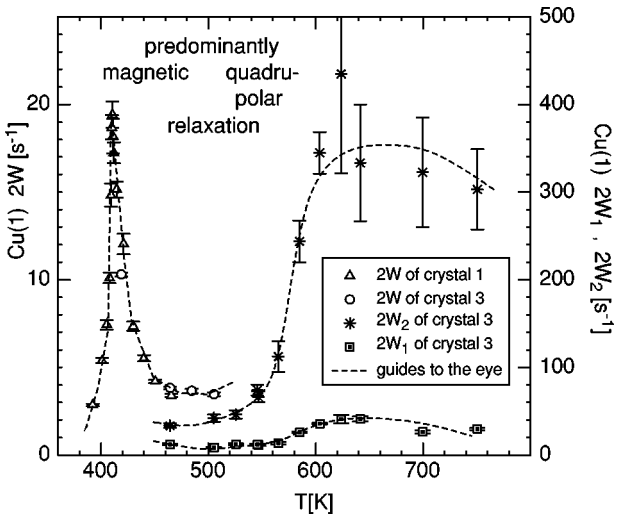

FIG. 7. Temperature dependence of the Cu(1) spin-lattice relaxation rate. $2W$, $2W_1$, and $2W_2$ are explained in the text. The dashed lines are guides to the eye.

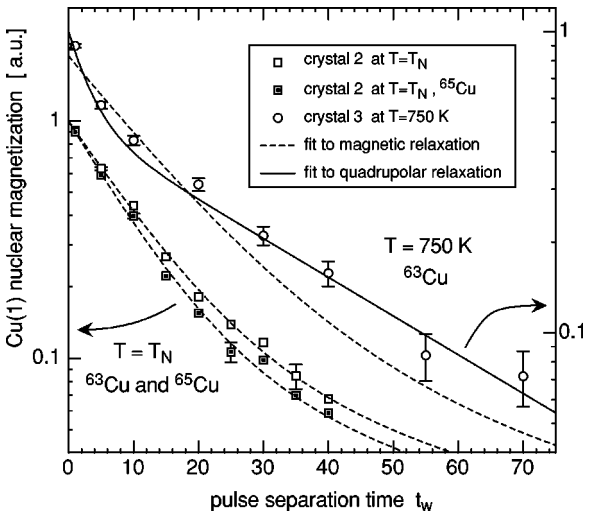

FIG. 9. Decay of the Cu(2) nuclear magnetization at T_N and 750 K. Dashed (solid) curves are fits to theoretical expressions for pure magnetic (quadrupolar) relaxation.

paired electron spin and, in addition, the transferred hyperfine coupling to the next ion with an unpaired electron spin is not too strong. The scaling behavior of Cu(1) and Cu(2) T_{1c} implies that in the temperature region below $T=470$ K Cu(1) is relaxed *magnetically* by the Cu(2) electron-spin fluctuations. This conclusion is supported by the following facts. First, the Cu(1) relaxation rates of the two Cu isotopes (^{63}Cu and ^{65}Cu) scale, within error bars, with the gyromagnetic ratios squared γ^2, which is what one expects from Eq. (7). Second, Fig. 9 shows that the magnetization recovery near T_N follows quite accurately the theoretical expression for *magnetic* relaxation, namely Eq. (6).

Next, the experimental ratio $T_{1c,\mathrm{Cu}(1)}/T_{1c,\mathrm{Cu}(2)}=2600$ is, according to Sec. III, equal to $(A_{ab}-4B)^2/2(B'_{ab})^2$. Together with $|A_{ab}-4B|=117$ kOe/μ_B (see above), the ratio yields $|B'_{ab}|=1.6$ kOe/μ_B which is our result for the Cu(1) hyperfine coupling constant due to one Cu(2) nearest neighbor. Since the direct dipolar field at the Cu(1) site produced by the AF ordered Cu(2) electron spins of one plane amounts to less than 100 Oe, the B'_{ab} coupling must predominantly arise from a *transferred* hyperfine field. This kind of coupling is in general positive and isotropic as will be confirmed, for the Cu(1) case, later.

The value we have obtained for $|B'_{ab}|$ may also be deduced from NQR measurements[44] of Lütgemeier *et al.* performed in a YBCO6 sample with 1% of Cu(1) replaced by Fe. The doping enforces, below T_N, a *ferromagnetic* order in the nearest CuO_2 planes (of the two adjacent bilayers) resulting in a nonzero magnetic field at the Cu(1) site, $B_{\mathrm{int}}=2.0$ kOe. Assuming that this field arises from just two magnetic moments of $\mu_{\mathrm{eff}}=0.68\mu_B$ magnitude (our value from above), the relation $B_{\mathrm{int}}=|2B'_{ab}|\mu_{\mathrm{eff}}$ yields $|B'_{ab}|=1.5$ kOe/μ_B, which agrees very well with our result.

One may wonder why the hyperfine interaction of the unpaired Cu(2) $3d_{x^2-y^2}$ electron spin with the Cu(1) nuclear spin is so strong although the shortest route for supertransfer via apex $2p_z$ orbital is not possible due to the orthogonality with Cu(2) $3d_{x^2-y^2}$ orbital. Obviously, there has to be another but more efficient transfer route. Perhaps, the unpaired electron from the Cu(2) $3d_{x^2-y^2}$ orbital polarizes first the two Cu(2) $3d_{3z^2-r^2}$ electrons as indicated in quantum-chemical calculations recently.[45] This would enable then the polarization supertransfer via apical oxygen $2p_z$ orbital and Cu(1) $4s$ shell to the Cu(1) nuclear spin. Of course, it remains to be shown that this is the right explanation.

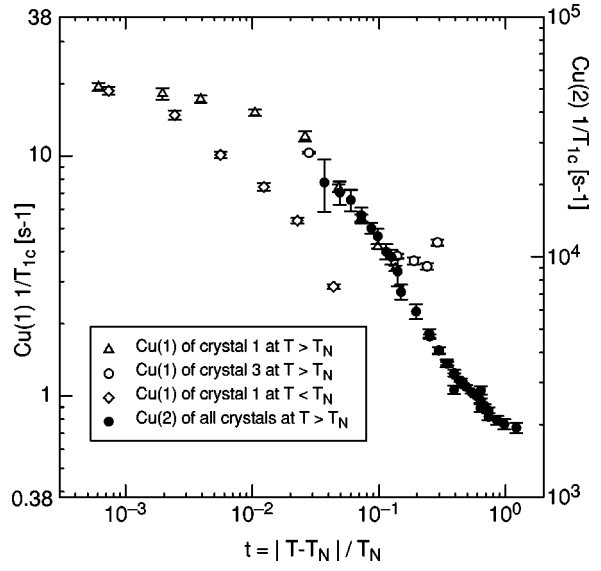

FIG. 8. The Cu(1) spin-lattice relaxation rates (for $\mathbf{B}_{\mathrm{ext}}\|c$) in both the paramagnetic and the ordered phase versus absolute value of the reduced temperature (open symbols). The full symbols denote Cu(2) rates above T_N.

2. Field dependence of T_N

Since the Cu(1) nuclei relax rather slowly, compared to Cu(2), one can measure T_{1c} and T_{1ab} of Cu(1) close to and even at T_N (Fig. 10). We identify the temperature where T_1 is minimal as the Néel temperature. In this way, we get T_N values that agree quite accurately with those gained from neutron-scattering experiments.[1]

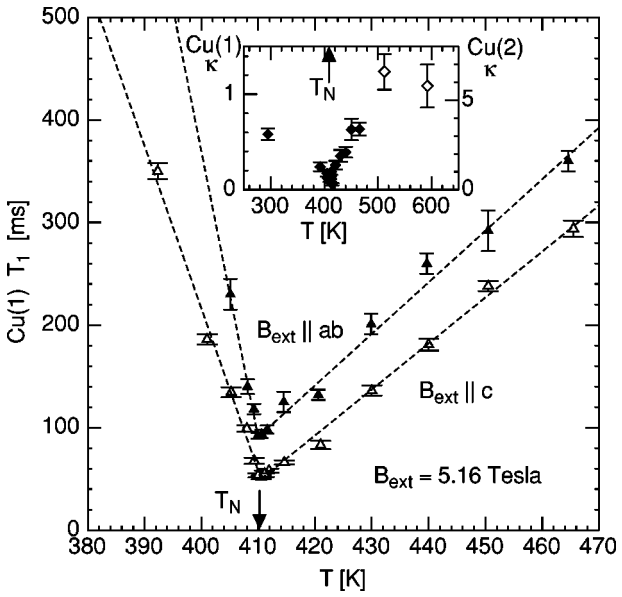

FIG. 10. Temperature dependence of the Cu(1) spin-lattice relaxation time in crystal 1 for $\mathbf{B}_{\text{ext}}\|c$ (open) and $\mathbf{B}_{\text{ext}}\|ab$ (full triangles). The dashed lines are guides to the eye. Inset: temperature dependence of the susceptibility anisotropy factor κ of Cu(1) (full) and Cu(2) (open diamonds).

Figure 10 also demonstrates that, within error bars, T_N of crystal 1 [410.3(5) K] does not depend on the orientation of the applied external magnetic field of 5.16 T. On the other hand, in the single-layer AF SCOCL, where T_N is only 257 K, T_N rises by several degrees when an external magnetic field is applied *parallel* to the CuO_2 planes while no effect is seen for $B_{\text{ext}}\|c$ (Ref. 8).

This difference can be understood as follows. For layered antiferromagnets, T_N is estimated by the mean-field relation

$$J'[\xi_{2\text{D}}(T_N)]^2 \approx kT_N, \tag{13}$$

where $[\xi_{2\text{D}}(T)]^2$ is approximately the number of short-range AF coupled spins that are present in a $\xi_{2\text{D}}a$ size spot. The energy gain per one AF coupled Cu pair sitting in an adjacent bilayer amounts to J'. When the exchange energy between two such neighboring spots in the adjacent bilayers surmounts kT, the system orders three-dimensionally.

As shown in Sec. IV A 2, the temperature dependence of $\xi_{2\text{D}}$ in the paramagnetic phase can be approximated by Eq. (12) where $\xi_{2\text{D}H}$ diverges at $T_N^{2\text{D}}=0$. An applied magnetic field parallel to the CuO_2 plane induces an additional Ising-like anisotropy that consequently raises the $\xi_{2\text{D}}$ divergence (or 2D ordering) temperature to a *finite* value.[8,46] Consequently, the in-plane correlation length increases more rapidly for decreasing temperature. However, in a field below 10 T this increase becomes noticeable only at temperatures below 300 K (Fig. 2 in Ref. 8) and thus influences only the low $T_N^{3\text{D}}$ of SCOCL but not the high Néel temperature of YBCO6.

One might wonder why the Néel temperatures of SCOCL and YBCO6 differ by more than 150 K although the J value in both AF amounts to 1450 K (Ref. 47). The answer is as follows. First, the interplane coupling in SCOCL is smaller[48] than in YBCO6 and, second, the bilayer correlation length increases much faster compared to the single-layer behavior (see Sec. IV A 4). According to Eq. (13), both differences contribute to the higher Néel temperature of YBCO6.

3. Dynamics near T_N

Obviously, the Cu(1) relaxation rate does not exhibit a 3D critical increase (characterized by the critical exponent $w\approx -0.33$) which one might expect to arise from the 3D critical slowing down of the Cu(2) electron-spin fluctuations at T_N (Fig. 8). Instead, in the paramagnetic as well as in the ordered phase, the Cu(1) rate seems to become ''flattened'' when the temperature approaches T_N.

The explanation of this behavior is as follows. One knows that due to symmetry no static internal field exists at the Cu(1) site in the *ordered* phase of YBCO6 (Ref. 16) because the hyperfine fields cancel. In the paramagnetic phase, when approaching T_N and a coupling of the bilayers sets in, one expects a similar cancellation of the fluctuating fields arising from spins of adjacent bilayers, leading to an increasing suppression or ''flattening''of the Cu(1) relaxation (see Fig. 8). This effect becomes noticeable at $|t|\approx 0.01$ (corresponding to $T_N\pm 4$ K) which agrees nicely with the T_N-2 K range where a recent neutron-scattering study[49] of the *ordered* phase detected a crossover from 2D to 3D behavior. Thus, the Cu(1) relaxation rate is rather a witness of growing AF coupling between the bilayers when T_N^+ is approached, but it is unable to mirror the Cu(2) 3D critical spin fluctuations.

4. Transition from XY to isotropic spin fluctuations

In Sec. IV A 6, we started to discuss the transition from XY-like spin fluctuations close to T_N to isotropic spin fluctuations far above T_N. Since the Cu(1) relaxation can be monitored very close to T_N, further information is obtained from the Cu(1) susceptibility anisotropy factor κ because the Cu(2) spin direction determines the direction of the hyperfine fields they generate at the Cu(1) site.

Cu(1) κ values are shown in the inset of Fig. 10 together with the two Cu(2) values measured above 500 K. In the temperature region $T_N\pm 5$ K, κ is 0.1(1) and hence $\chi_c'' \ll \chi_{ab}''$. In others words, the Cu(2) spin fluctuations are strongly suppressed in the c direction. This is a consequence of the in-plane anisotropy, $J_{xy}\approx 10^{-4}J$ (Ref. 1), which is, in the ordered state, also responsible for the spin alignment parallel to the CuO_2 plane. With increasing temperature, there is a continuous crossover from anisotropic to isotropic Cu(2) spin fluctuations indicated by a growing κ, reaching a 0.65(10) value at 460 K. Recently, we observed a similar crossover in CASCO (Ref. 34) and it had been reported also for SCOCL.[8]

At sufficiently high temperature, the Cu(1) κ should approach the constant value $(g_c/g_{ab})^2=1.2$ (see Sec. III) provided both the spin-fluctuation and the hyperfine coupling constant $B'_{\alpha\alpha}$ are isotropic. However, if the hyperfine coupling were purely dipolar, κ would reach a much larger limiting value, namely $(B'_{c,\text{dip}}/B'_{ab,\text{dip}})^2(g_c/g_{ab})^2=[2/(-1)]^2 1.2=4.8$. Unfortunately, the Cu(1) $1/T_1$ anisotropy gets spoiled above 500 K by a strong additional quadrupolar relaxation contribution having its own anisotropy unrelated to spin fluctuations. From our *plane* Cu(2) anisotropy values, we concluded before that the transition to pure isotropic spin fluctuations is completed already at about 500

K. Therefore, one may say that the moderate increase of the Cu(1) κ value above T_N favors an isotropic hyperfine coupling constant B' rather than an anisotropic dipolar one.

For comparison, the inset of Fig. 10 also shows our κ value for the ordered phase, namely at 300 K, where we measured $T_{1c}/T_{1ab}=1.39(2)$ s / 1.76(4) s $=0.79(3)$, thus yielding $\kappa=0.58(6)$ which is very close to the 460 K value in the paramagnetic phase.

5. Quadrupolar relaxation beyond 500 K

Next, we discuss the crossover from magnetic relaxation at temperatures below 500 K (see Sec. IV C 1) to quadrupolar relaxation, due to diffusing chain oxygen, at higher temperatures. Figure 9 shows that the magnetization recovery at 750 K disagrees clearly with magnetic relaxation [Eq. (6)], but follows quite accurately the theoretical expression for quadrupolar relaxation, namely Eq. (10). This result confirms the finding of Matsumura *et al.*[21] that, at temperatures above 530 K, the Cu(1) relaxation rate is proportional to the Cu quadrupole moment squared, a clear sign of pure quadrupolar relaxation.

Figure 7 provides an overview of the relaxation rates $2W$, $2W_1$, and $2W_2$. Apparently, the temperature of 500 K marks the transition between dominating magnetic and quadrupolar relaxation, respectively. Both quadrupolar rates, $2W_1$ and $2W_2$, rapidly increase above 500 K and exhibit a maximum or saturation around 650 K. The ratio of $2W_2/2W_1=9$ at 600 K contains information about the excitation modes of the lattice vibration at the Cu(1) site caused by diffusing chain oxygen and allows, in principle, to test different models of diffusion of remnant chain oxygen.

The saturation of the Cu(1) rate around 650 K has *not* been observed by Matsumura *et al.*[21] who studied the Cu(1) relaxation in a YBCO6 powder sample with $T_N=415$ K, i.e., in a sample with even smaller chain oxygen content. The authors reported a rate increase up to $1/T_1=5\times10^4$ s^{-1} (at 780 K), a value which is about 150 times larger than the highest $2W_2$ rate we measured. Matsumura *et al.* interpreted their data, which follow an Arrhenius law over three decades, as the result of oxygen diffusion and extracted a diffusion activation energy of 1.15 eV. As it is obvious from Fig. 7, our data exhibit a rather different behavior. At present, there is no explanation for this difference.

D. Cu(1) magnetic shift and linewidth

The temperature dependence of the Cu(1) K_c data (Fig. 11) is similar to that of the static spin susceptibility[20,42,43] and does not reveal any anomaly at T_N. As already stated above, the Cu(1) ion does not have an unpaired electron spin. So, there is no on-site contribution to the spin part of the magnetic shift and since the orbital part $K_{\rm orb}$, is temperature independent, the temperature dependence of Cu(1) K_c must arise from the transferred hyperfine fields generated by the plane Cu(2) electron spins. Cu(1) K_c consequently should reflect the spin susceptibility of the planes, $\chi_0(T)$.

From the sign of the slope of the Cu(1) magnetic shift, $dK_c^{\rm exp}/dT$, which is positive, one can determine, with the help of Eqs. (4) and (5), the sign of the transferred hyperfine coupling, B', using the relation $dK^{\rm exp}/dT=dK^{\rm spin}/dT=2B'd\chi_0/dT$. Since $d\chi_0/dT>0$, it follows that B' has to be positive too. The same positive sign is obtained[22,36] for the Cu(2) in-plane *transferred* hyperfine coupling constant B, a property that seems to be typical for this kind of coupling mechanism.

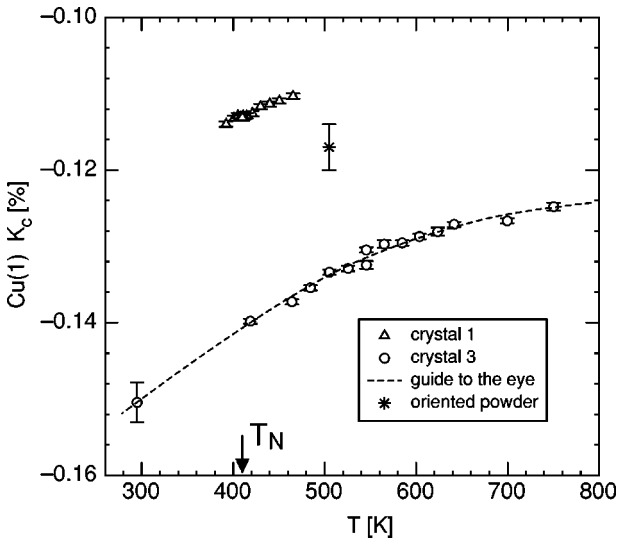

FIG. 11. Temperature dependence of the Cu(1) magnetic shift for $\mathbf{B}_{\rm ext}\|c$. The dashed line is a guide to the eye.

Since the Cu(1) linewidth (not shown here) of different specimens varies by a factor of 2, it is, similar to the Cu(2) linewidth, not an intrinsic parameter but depends on the quality of the individual crystals. For example, the Cu(1) linewidth in crystal 1 (as determined by Fourier transform of the free induction decay) is 5.5 kHz (for $\mathbf{B}_{\rm ext}\|c$) and independent of temperature between T_N and 470 K. At T_N, the linewidth slightly increases and seems to remain 7 kHz down to 390 K, the lowest temperature point measured. Also the Y linewidth[50] remains constant above T_N but increases strongly below T_N so that it doubles at $\approx$370 K. At the $\mathbf{B}_{\rm ext}\|ab$ orientation, the Cu(1) linewidth values scatter too much to allow one to resolve any temperature dependence.

E. Increase of the Y relaxation rate due to bilayer decoupling

Alloul *et al.*[51] have reported ^{89}Y spin-lattice relaxation data obtained from a YBCO6 powder sample. Above 425 K, the authors observed an *increase* of the Y rate that contrasts to the decreasing $1/T_1$ of the neighboring Cu(2) nuclei which relax through the strong Cu(2) spin fluctuations.

On the other hand, the Y temperature dependence is quite similar to our Cu(1) relaxation data in that temperature range, tempting to make the chain oxygen diffusion responsible for the Y relaxation as well. However, this possible source for the unusual Y relaxation enhancement can be excluded for two reasons. First, Y nuclei having $I=1/2$ and, therefore, no quadrupole moment, do not sense electric charge fluctuations caused by diffusing oxygen. Second, any possible magnetic relaxation induced by the same oxygen diffusion would be too weak due to the large Y-Cu(1) distance and the very small ^{89}Y magnetic moment.

Two other possibilities to explain the increase of Y $1/T_1$ are the following: (i) the high-temperature enhanced contribution from spin fluctuations with wave vectors far away from $Q_{\rm AF}$ predicted by Chakravarty *et al.*[52] and verified by

Thurber *et al.*[9] using ^{17}O $1/T_1$ in paramagnetic SCOCL; (ii) the decoupling of the two planes in the bilayer (Sec. IV A 4) taking place at ≈ 500 K. We will discuss possibility (ii) in more detail.

Above 500 K, the dipolar fields arising from the two CuO_2 planes do not cancel anymore at the Y site as they do in the case of AF coupled planes within the bilayer. Thus, these dipolar fields now contribute to the Y relaxation; this extra contribution is estimated as follows. The four AF correlated NN Cu(2) spins from one plane produce a dipolar hyperfine field at the Y site which we calculated with the help of the well-known structure data [$a=b=3.86$ Å, interplane distance $=3.33$ Å, Ref. 19]. The coupling constants specifying the dipolar field are $D_{ab}^{\rm dip}=1.24$ kOe/μ_B and $D_c^{\rm dip}=0$. Using the relation $1/T_{1c} \propto \gamma_n^2[A_{ab}^{\rm spin}(\mathbf{Q_{AF}})]^2$ (Sec. III), and the $^{63}Cu(2)$ relaxation rate at 600 K, $1/^{63}T_{1c}=3000$ s^{-1}, we get for the Y relaxation rate: $1/^{89}T_{1c}=(^{89}\gamma/^{63}\gamma)^2[2D_{ab}^2/(A_{ab}-4B)^2](1/^{63}T_{1c})=0.023$ s^{-1}. This result is of the same order of magnitude as the experimental *increase* of 0.07 s^{-1} of the Y relaxation rate between T_N and 600 K. Thus, the observed increase of the Y relaxation rate above 425 K is, at least partially, due to the magnetic decoupling of the planes of the bilayer.

V. SUMMARY

We have reported a detailed Cu NMR study of high-quality $YBa_2Cu_3O_{6.12}$ single crystals in their paramagnetic phase, ranging from slightly below $T_N \cong 410$ K up to nearly 1000 K. The temperature dependence of the Cu(1) and Cu(2) spin-lattice relaxation rates and their anisotropies and the magnetic shift in *c* direction at both sites have been measured. The major results obtained in the various temperature regimes are as follows.

Above 500 K, the Cu(2) relaxation data reveal that $YBa_2Cu_3O_{6.12}$ is in the renormalized classical regime of a 2D quantum Heisenberg antiferromagnet (AF) with spin $S=1/2$, what means that electron spins of neighboring planes fluctuate independently. From the data, we calculated the temperature dependence of the AF correlation length and determined a value for the hyperfine coupling constant at the Cu(2) site, $|A_{ab}-4B|=117(3)$ kOe/μ_B, and the effective magnetic moment, $\mu_{\rm eff}=0.68(2)\mu_B$. Thus, among the antiferromagnets La_2CuO_4, $YBa_2Cu_3O_6$, and $(Ca,Sr)CuO_2$, the value of the effective magnetic moment is larger the stronger the magnetic interplane coupling. Above 600 K, the Cu(2) hyperfine coupling constant (A_c+4B) exhibits an unusual change which is not yet explained. The Cu(1) hyperfine coupling constant due to one Cu(2) nearest neighbor, is $B'=1.6$ kOe/μ_B; it is positive and approximately isotropic. Finally, we inferred, from the Cu(1) relaxation above 500 K, that diffusion of remnant oxygen in the chains is present.

Below 500 K, the individual layers in $YBa_2Cu_3O_{6.12}$ start to couple into pairs and the temperature dependence of the AF correlation length abruptly crosses over to a faster increase when T_N is approached. The corresponding effective AF in-plane coupling constant becomes $J_{\rm eff}=4100$ K, a value nearly three times larger than $J=1450$ K known for the isolated layer. A comparison with quantum Monte Carlo calculations allows one to estimate an intrabilayer coupling constant, $J_b/J \lesssim 0.01$, which is significantly smaller than $J_b/J=0.08$ as obtained by neutron-scattering experiments. The origin of this disagreement is not yet known. Only ≈ 4 K above T_N, do the bilayers begin to couple as indicated by a suppression of the Cu(1) relaxation rate. The decoupling of the planes adds to the increase of the ^{89}Y relaxation rate above 425 K.

Measuring the susceptibility anisotropy, we detected a crossover in the Cu(2) spin fluctuations. In the range $T_N \pm 5$ K, these fluctuations are *XY*-like and become, with rising temperature, approximately isotropic; the crossover is already complete around 500 K. This behavior is similar to the crossover we observed recently in $(Ca,Sr)CuO_2$.

The Néel temperature of $YBa_2Cu_3O_{6.12}$ does not depend on the orientation of the applied magnetic field of 5.16 T. This behavior contrasts with that of $Sr_2CuO_2Cl_2$ where the orientational dependence of T_N is a consequence of its low value, namely 257 K.

ACKNOWLEDGMENTS

We thank H. Schwer for performing the x-ray-diffraction measurements, D. Schnarwiler and B. Nussberger for preparing and sealing the quartz ampoules, and K. Bösiger and B. Schmid for high-precision machine work on the sample holders and the probehead. We are grateful for very stimulating discussions with A. Zavidonov, A. Suter, and J. Roos. This work was supported in part by the ''Schweizerischer Nationalfonds.''

[1] J. Rossat-Mignod, L. P. Regnault, P. Burlet, C. Vettier, and J. Y. Henry, in *Selected Topics in Superconductivity*, edited by L. Gupta and M. Multani (World Scientific, Singapore, 1993).

[2] K. Yamada, K. Kakurai, Y. Endoh, T.R. Thurston, M.A. Kastner, R.J. Birgeneau, G. Shirane, Y. Hidaka, and T. Murakami, Phys. Rev. B **40**, 4557 (1989).

[3] M. Greven, R.J. Birgeneau, Y. Endoh, M.A. Kastner, B. Keimer, M. Matsuda, G. Shirane, and T.R. Thurston, Phys. Rev. Lett. **72**, 1096 (1994).

[4] F. Borsa, M. Corti, T. Goto, A. Rigamonti, D.C. Johnston, and F.C. Chou, Phys. Rev. B **45**, 5756 (1992).

[5] T. Imai, C.P. Slichter, K. Yoshimura, and K. Kosuge, Phys. Rev. Lett. **70**, 1002 (1993).

[6] T. Imai, C.P. Slichter, K. Yoshimura, M. Katoh, and K. Kosuge, Phys. Rev. Lett. **71**, 1254 (1993).

[7] M. Matsumura, H. Yasuoka, Y. Ueda, H. Yamagata, and Y. Itoh, J. Phys. Soc. Jpn. **63**, 4331 (1994).

[8] B.J. Suh, F. Borsa, L.L. Miller, M. Corti, D.C. Johnston, and D.R. Torgeson, Phys. Rev. Lett. **75**, 2212 (1995).

[9] K.R. Thurber, A.W. Hunt, T. Imai, F.C. Chou, and Y.S. Lee, Phys. Rev. Lett. **79**, 171 (1997).

[10] P. Hasenfratz and F. Niedermeyer, Phys. Lett. B **268**, 231 (1991).

[11] S. Chakravarty and R. Orbach, Phys. Rev. Lett. **64**, 224 (1990).

[12] L. Yin, M. Troyer, and S. Chakravarty, Europhys. Lett. **42**, 559 (1998).

[13] A.W. Sandvik and D.J. Scalapino, Phys. Rev. B **53**, R526 (1996).

[14] A. Erb, E. Walker, and R. Flükiger, Physica C **245**, 245 (1995).
[15] A. Erb, E. Walker, and R. Flükiger, Physica C **258**, 9 (1996).
[16] H. Yasuoka, T. Shimizu, T. Imai, and S. Sasaki, Hyperfine Interact. **49**, 167 (1989).
[17] S.M. Hayden, G. Aeppli, T.G. Perring, H.A. Mook, and F. Dogan, Phys. Rev. B **54**, R6905 (1996).
[18] T.B. Lindemer *et al.*, J. Am. Ceram. Soc. **72**, 1775 (1989).
[19] H. Schwer, ETH Zürich (private communication).
[20] Y. Yamaguchi, M. Tokumoto, S. Waki, Y. Nakagawa, and Y. Kimura, J. Phys. Soc. Jpn. **58**, 2256 (1989).
[21] M. Matsumura, T. Shiohara, and H. Yamagata, J. Phys. Soc. Jpn. **67**, 3267 (1998).
[22] F. Mila and T.M. Rice, Physica C **157**, 561 (1989).
[23] E. Andrew and D. Tunstall, Proc. Phys. Soc. London **78**, 1 (1961).
[24] T. Moriya, J. Phys. Soc. Jpn. **18**, 516 (1963).
[25] A.J. Millis, H. Monien, and D. Pines, Phys. Rev. B **42**, 167 (1990).
[26] J.A. Arambu and M. Moreno, J. Chem. Phys. **83**, 6071 (1985).
[27] D. Shaltiel, H. Bill, P. Fischer, M. Francois, H. Hagemann, M. Peter, Y. Ravi Sekhar, W. Sadowski, H.S. Scheel, G. Triscone, E. Walker, and K. Yvon, Physica C **158**, 424 (1989).
[28] M. Gordon and M. Hoch, J. Phys. C **11**, 783 (1978).
[29] K. Yosida and T. Moriya, J. Phys. Soc. Jpn. **11**, 33 (1956).
[30] C. P. Slichter, *Principles of Magnetic Resonance* (Springer, Berlin, 1992).
[31] M. Mali, I. Mangelschots, H. Zimmermann, and D. Brinkmann, Physica C **175**, 581 (1991).
[32] A. Lombardi, M. Mali, J. Roos, D. Brinkmann, and I. Mangelschots, Phys. Rev. B **54**, 93 (1996).
[33] R. Navarro and L.J. de Jongh, Physica B **98**, 1 (1979).
[34] R. Pozzi, M. Mali, M. Matsumura, F. Raffa, J. Roos, and D. Brinkmann, Phys. Rev. B **56**, 759 (1997).
[35] A. Sokol, E. Gagliano, and S. Bacci, Phys. Rev. B **47**, 14 646 (1993).
[36] Y. Zha, V. Barzykin, and D. Pines, Phys. Rev. B **54**, 7561 (1996).
[37] A.V. Chubukov and S. Sachdev, Phys. Rev. Lett. **71**, 169 (1993).
[38] M.P. Gelfand and R.R.P. Singh, Phys. Rev. B **47**, 14 413 (1993).
[39] S.E. Barrett, D.J. Durand, C.H. Pennington, C.P. Slichter, T.A. Friedmann, J.P. Rice, and D.M. Ginsberg, Phys. Rev. B **41**, 6283 (1990).
[40] M. Bankay, M. Mali, J. Roos, and D. Brinkmann, Phys. Rev. B **50**, 6416 (1994).
[41] S. Ohsugi, Y. Kitaoka, K. Ishida, G. Zhang, and K. Asayama, J. Phys. Soc. Jpn. **63**, 700 (1994).
[42] K. Westerholt and H. Bach, Phys. Rev. B **39**, 858 (1989).
[43] R. Navarro, in *Magnetic Properties of Layered Transition Metal Compounds*, edited by L.J. de Jongh (Kluwer, Dordrecht, 1990), p. 105.
[44] H. Lütgemeier, R.A. Brand, Ch. Sauer, B. Rupp, P.M. Meuffels, and W. Zinn, Physica C **162-164**, 1367 (1989).
[45] E.P. Stoll, P. Hüsser, and P.F. Meier (private communication).
[46] H.-Q. Ding, Phys. Rev. Lett. **68**, 1927 (1992).
[47] Y. Tokura, S. Koshihara, T. Arima, H. Takagi, S. Ishibashi, T. Ido, and S. Uchida, Phys. Rev. B **41**, 11 657 (1990).
[48] T. Yildirim, A.B. Harris, O. Entin-Wohlman, and A. Aharony, Phys. Rev. Lett. **72**, 3710 (1994).
[49] W. Montfrooij, H. Casalta, P. Schleger, N.H. Anderson, A.A. Zhokov, and A.N. Christensen, Physica B **241-243**, 848 (1998).
[50] T. Ohno, H. Alloul, and P. Mendels, J. Phys. Soc. Jpn. **59**, 1139 (1990).
[51] H. Alloul, J. Appl. Phys. **69**, 4513 (1991).
[52] S. Chakravarty, M.P. Gelfand, P. Kopietz, R. Orbach, and M. Wollensak, Phys. Rev. B **43**, 2796 (1991).
[53] From the fit of Eqs. (11) and (12) to the data between 400 and 600 K of Ref. 7 as described in Sec. IV A 2.
[54] T. Tsuda, T. Shimizu, H. Yasuoka, K. Kishio, and K. Kitazawa, J. Phys. Soc. Jpn. **57**, 2908 (1988).
[55] H. Yasuoka, T. Shimizu, Y. Ueda, and K. Kosuge, J. Phys. Soc. Jpn. **57**, 2659 (1988).